Lab on a Chip

# Fluorophilic Boronic Acid Copolymer Surfactant for Stabilization of Complex Emulsion Droplets with Fluorinated Oil



| | |
|---|---|
| Journal: | *Lab on a Chip* |
| Manuscript ID | LC-COM-03-2025-000309.R1 |
| Article Type: | Communication |
| Date Submitted by the Author: | 13-Apr-2025 |
| Complete List of Authors: | Wu, Zhang; Harvard University, School of Engineering and Applied Sciences<br>Deveney, Brendan; Harvard University,<br>Werner, Jörg; Boston University, Mechanical Engineering<br>Aime, Stefano; ESPCI Paris, C3M<br>Weitz, David; Harvard University, Department of Physics |
| | |

COMMUNICATION

# Fluorophilic Boronic Acid Copolymer Surfactant for Stabilization of Complex Emulsion Droplets with Fluorinated Oil

Zhang Wu,[a] Brendan T. Deveney,[a] Jörg G. Werner,*[b] Stefano Aime [c] and David A. Weitz *[ad]

Received 00th January 20xx,
Accepted 00th January 20xx

DOI: 10.1039/x0xx00000x

**A fluorosurfactant is synthesized by the copolymerization of fluoroacrylate and boronic acid acrylamide monomers to stabilize fluorinated oil droplets. The copolymer surfactant couples with diols or polyols in adjacent aqueous phase to form an ultrathin elastic interfacial film to rigidify the interface, thereby preventing drop recoalescence and enabling new applications.**

## 1. Introduction

Droplet formation and stabilization are essential steps for droplet-based techniques across multiple fields such as materials science, pharmaceuticals, and biotechnology[1-3]. Manipulating liquid-liquid interfaces is important for the formation of stable emulsions. Surfactants that are amphiphilic molecules with hydrophilic and hydrophobic components favoring different phases, adsorb onto the droplet interface and prevent the drop coalescence, therefore kinetically stabilizing emulsion droplets[4-9]. A variety of surfactants have been designed and synthesized for diverse applications to stabilize droplet interfaces between two immiscible liquids, typically water and a hydrophobic oil[10-12]. By contrast, there are far fewer surfactants for fluorinated oils; these oils exhibit chemical inertness and biocompatibility, which are important for biochemical reactions and various biological applications[13-18]. Additionally, unlike hydrocarbon oils, the fluorinated oils have good compatibility with polydimethylsiloxane, and are therefore widely used in microfluidic devices prepared by soft lithography[19-22]. Commonly available fluorosurfactants, including perfluorooctanoic acid, perfluorooctanesulfonic acid and perfluoropolyether derivatives cannot effectively stabilize the droplets, which is important for technologies such as digital PCR or the fabrication of complex emulsions containing fluorocarbon[23].

Of particular interest for advanced stimuli-responsive or dynamic complex fluids are mixtures of liquid hydrocarbons and fluorocarbons that exhibit temperature-dependent miscibility[24-25], which has been utilized for the fabrication of thermally reconfigurable emulsions[26]. For example, single emulsion droplets consisting of hydrocarbon and fluorocarbon oils dispersed in an aqueous continuous phase reversibly reconfigure into a hydrocarbon-in-fluorocarbon-in-water double emulsion structure upon cooling below their upper critical solution temperature (UCST). Furthermore, transitions between double emulsion and Janus droplet morphologies have been achieved by changing the surfactants in the continuous phase to tune the balance between the interfacial tensions of the various fluid combinations. The control over the arrangement of the liquid interfaces in a complex emulsion droplet has opened new directions for droplet-based applications such as microsensors and liquid lenses[27-37]. However, fabrication and permanent stabilization of reconfigurable hydrocarbon-fluorocarbon emulsions with higher complexity remain elusive. Therefore, the development of a fluorosurfactant to improve the droplet stability would be of great importance for the design and application of advanced reconfigurable emulsions across multiple complexities and broadening their potential as responsive materials.

In this work, we introduce a tunable fluorophilic boronic acid (FBA) copolymer surfactant which can rigidify the water/fluorinated oil interface to stabilize complex hydrocarbon-fluorocarbon-water emulsions. The FBA copolymer couples with diols or polyols such as poly(vinyl)

[a] John A. Paulson School of Engineering and Applied Sciences, Harvard University, Cambridge MA.
[b] Department of Mechanical Engineering and Division of Materials Science and Engineering, Boston University, Boston, Massachusetts 02215, USA.
[c] Ecole Supérieure de Physique et de Chimie Industrielles (ESPCI), Paris.
[d] Department of Physics, Harvard University, Cambridge MA, USA.

alcohol (PVA) dissolved in the aqueous phase through dynamic boronic ester bonds (Figure 1a). The coupling of the two produces a solid elastic interfacial film on the water-oil interfaces, thereby enabling the stabilization of complex emulsions droplets containing fluorinated oils and their mixtures. For example, water-in-oil-in-water double emulsion drops featuring a shell composed of thermally responsive hydrocarbon and fluorocarbon oil mixtures are rendered stable. Temperature-induced phase separation of the two oil components confined within the double emulsion shells leads to a complex morphological reconfiguration of the two-component double emulsion to three-component triple emulsion drops. These results highlight the value of this new FBA fluorosurfactant.

## 2. Materials and Methods

**Synthesis of FBA Copolymer**

A mixture of azobisisobutyronitrile (AIBN; 0.0301 g), N-[3-(4,4,5,5-tetramethyl-1,3,2-dioxaborolan-2-yl)phenyl] acrylamide (0.2 g) and 1H,1H,2H,2H-heptadecafluorodecyl acrylate (0.9271 mL) in dimethylformamide (DMF; 3.44 mL) is degassed by bubbling with nitrogen and stirred under inert conditions at 70 ºC for 48 hours. The solution typically turns turbid within an hour. The product is washed by repeatedly precipitating the mixture in an excess of methanol, centrifuging, and decanting the supernatant. After the final decanting step, the polymer is dried in a vacuum oven at ~70 ºC overnight. After the polymer has dried, it is added to a ~1M solution of hydrochloric acid (15 mL) and stirred overnight at 100 ºC under reflux to remove the pinacol protecting group of the boronic acid component of the polymer. Following deprotection, the polymer is again precipitated and washed in an excess of methanol. After purification, the polymer is dried overnight in a vacuum oven at ~70 ºC. The polymer is then mixed with PFH (3-5 wt%) and stirred with heating at 60 ºC, typically overnight, to disperse the polymer. After the polymer is dispersed, the dispersion is filtered with a 1-2 micron filter and the filtrate is used for drop-making.

**Characterization of the FBA-PVA Interfacial Properties**

The surface tensions of the interfaces are characterized using pendant drop method on the droplet lab tensiometer and analyzed with the OpenDrop package available at https://github.com/jdber1/opendrop. To assess the rheological properties of the FBA-PVA interfacial film, we use HR 20 discovery hybrid rheometer by TA instruments, which is equipped with a double wall ring performing interfacial rheology to probe the complex shear modulus of the interface[38-39]. Oscillatory amplitude sweep is carried out at oscillation strain from 0.1% to 10% and angular frequency of 10.0 rad/s. Oscillatory frequency sweep is conducted at angular frequency from 1.0 to 100 rad/s and strain of 1.0% in the LVE region.

**Fabrication and Characterization of the Reconfigurable Double Emulsions**

Droplet-based microfluidics method is employed for the drop generation of the reconfigurable double emulsions. Oil mixtures of hexane and PFH at 1:1 volume ratio, combined with FBA polymer at 3-5 wt% are injected as middle phase into the glass capillary microfluidic device[40-44], interfacing with the inner and outer phases of 10 wt% PVA aqueous solutions to form double emulsions, as depicted in Figure 4a. The double emulsions are then collected and placed onto a temperature control stage for imaging with confocal microscopy. Bright-field and fluorescent confocal micrographs of the microcapsules are captured for the characterization of the droplet morphologies at room temperature and ~0 ºC, respectively. The phase separation in the shell during the high-to-low temperature transition is captured by confocal time-lapse imaging.

## 3. Results and Discussion

The polymeric FBA surfactant is synthesized by the copolymerization of a perfluoro-acrylate and boronic acid acrylamide, whose chemical structure is depicted in Figure 1b. Due to the presence of a majority of perfluorinated acrylate monomer, the FBA copolymer is soluble in common fluorinated oils such as perfluorohexane (PFH) and HFE-7500. The boronic acid group of the copolymer can couple with diols or polyols through dynamic covalent boronic ester bonds that act like a key-and-lock mechanism when combined at an interface of such fluorinated oils and water, as depicted in Figure 1a. The interfacial crosslinking of the FBA copolymer in the fluorinated oil phase with the PVA surfactant in the water phase results in the formation of an elastic interfacial film, which prevents drop coalescence by enforcing elastic collisions between the droplets, as depicted in Figure 1c. Unlike commonly used fluorosurfactants that produce liquid droplet interfaces, the FBA surfactant rigidifies the water/oil interface and increases interfacial elasticity, making the droplets more resistant to physical disturbances and thereby enhancing their stability. The interfacial coupling between FBA in the PFH phase and the hydroxyl groups of PVA in the water phase is visualized by the transient wrinkle formation during retraction of the PFH droplet from the water, as shown in Figure 2a and Supporting Video SV1. This demonstrates the formation of a solid elastic interfacial film in the presence of both components. The slow disappearance of the wrinkles and return of the drop to its original shape confirms the dynamic nature of the boronic ester bonds.

To evaluate the impact of the FBA and PVA components on the interface between water and fluorinated oils, their interfacial tension is quantified using the pendant drop method. The addition of FBA to PFH reduces the interfacial tension of the PFH-water interface to around 20 mN $m^{-1}$, as compared to ~30 mN $m^{-1}$ without any additives; moreover, the addition of PVA to

 

water reduces the interfacial tension of the PFH-water interface to around 17 mN $m^{-1}$, as shown in Figure 2b-c. A similar surface tension is obtained when using the combination of FBA-in-PFH and PVA-in-water. However, lasting stabilization against coalescence of fluorocarbon-water emulsions is only obtained for the combined FBA-PVA system, not when only the individual components are used. This indicates that the synergistic and beneficial interfacial assembly of the FBA and PVA is necessary for stabilization.

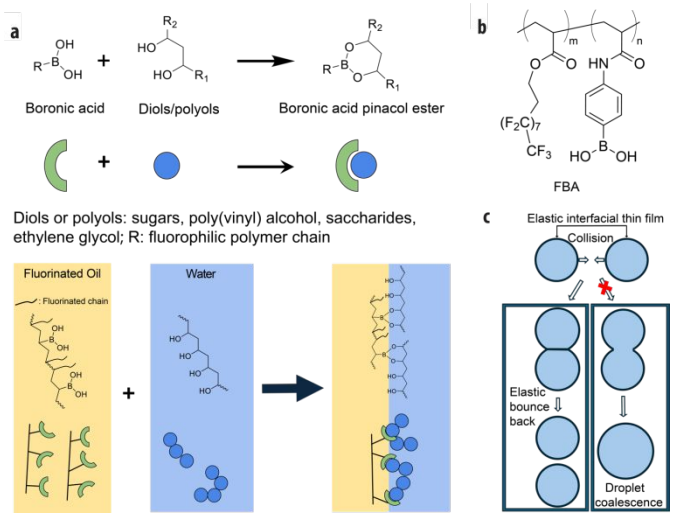


**Figure 1.** (a) Reaction of boronic acid with diols or polyols such as sugars, poly(vinyl) alcohol, saccharides, and ethylene glycol to form boronic acid pinacol ester (top); coupling mechanism of the FBA copolymer in the oil phase with PVA in the water phase at the interface (bottom). (b) Chemical structure of the FBA copolymer. (c) Schematic representation of droplet stabilization by interfacial crosslinking between the FBA copolymer and PVA that leads to the formation of an elastic interfacial thin film to prevent drop coalescence.

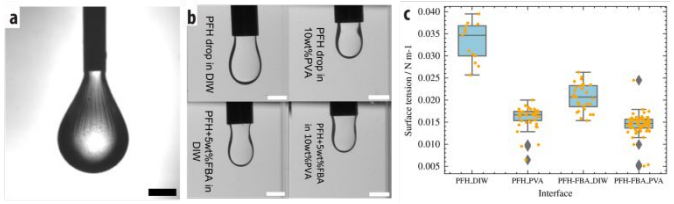


**Figure 2.** (a) Transient wrinkle formation during retraction of hydrofluoroether 7500 (HFE-7500) drop containing 3 wt% FBA copolymer from a water bath consisting of 0.08 M 4-(2-hydroxyethyl)-1-piperazineethanesulfonic acid (HEPES) and 2 wt% PVA. Scale bar is 500 μm. (b-c) Selected pendant drop tensiometry captured grayscale images (b) and surface tension measurements (c) for PFH-water drop interfaces with and without the addition of FBA in PFH phase or PVA in deionized-water (DIW) phase. All scale bars are 2 mm. Boxplots show the distribution of surface tension values for the PFH/ DIW, PFH/ PVA-water, PFH+FBA/ DIW, and PFH+FBA/ PVA-water (from left to right) interfaces. Orange dots represent individual data points, and gray diamonds indicate outliers. The boxes indicate the interquartile range (IQR), with the horizontal line inside representing the median surface tension value, and the two lines outside the box extended to the maximum and minimum values for each condition.

Amplitude and frequency sweeps of interfacial rheology are conducted to probe the complex shear modulus for HFE-7500 and water interfaces with different fluorosurfactant systems. As compared to the shear modulus of the interfaces with 008-FluoroSurfactant from RAN biotechnologies, PVA or none as a control, the FBA-PVA interface exhibits a two orders of magnitude higher complex shear modulus, as shown in Figure 3a, c. At low deformations, the storage and loss moduli of the FBA-PVA remain constant in the linear-viscoelastic (LVE) region, as shown by the amplitude sweep of the FBA-PVA interface in Figure 3b; at low frequencies, the storage and loss moduli of the FBA-PVA also remain constant in the LVE region, as shown by the frequency sweep of the FBA-PVA interface in Figure 3d. Both the amplitude and frequency sweeps show that the storage modulus is larger than the loss modulus, indicating that the FBA-PVA interface behaves more like a viscoelastic solid. The frequency sweep of the FBA-PVA interfacial film with dynamic covalent-bonding also shows a marked shear-thinning behavior, indicated by a decrease in complex viscosity with increasing frequency, as shown in Figure 3d. At higher strain rates, dynamic bonds may break more rapidly than they can reform, leading to shear thinning behavior[45-46]. This nonlinear rheological property is common in soft materials with reversible bonding such as self-healing hydrogels and supramolecular polymer networks[47-50].

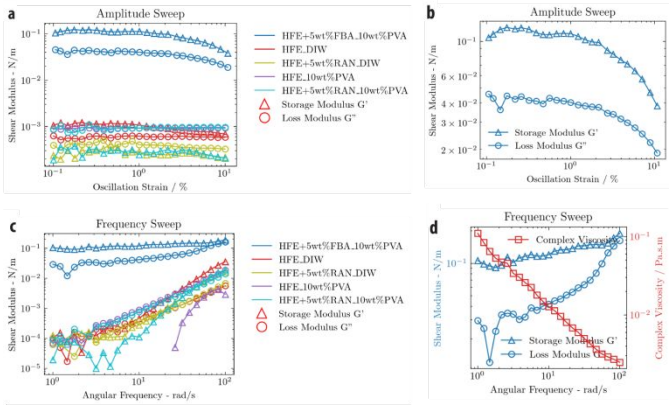


**Figure 3.** (a) Oscillatory amplitude sweeps at oscillation strain from 0.1% to 10% and angular frequency of 10.0 rad/s for HFE-7500 and water interfaces with different surfactants. The storage modulus of the interface of HFE-7500 with 10 wt% PVA is beyond the detection limit of the interfacial rheometer, therefore not shown in the plot. (b) Zoom - in plot of the amplitude sweep result for the interface of HFE - 7500+5 wt% FBA with 10 wt% PVA (right). (c) Oscillatory frequency sweep at

angular frequency from 1.0 to 100 rad/s and strain of 1.0% in the LVE region for HFE-7500 and water interfaces with different surfactants. HFE-7500 and water interfaces with 008-FluoroSurfactant from RAN biotechnologies, PVA or none are used for control experiments. (d) Zoom - in plot of the amplitude frequency result with complex interfacial viscosity of HFE-7500 + 5 wt% FBA with 10 wt% PVA (right).

To demonstrate it utility, we apply the FBA: PVA surfactant system to the fabrication of complex reconfigurable hydrocarbon-fluorocarbon emulsions. Double emulsion droplets consisting of a water core and an oil shell comprised of a 1:1 hexane: PFH mixture are fabricated using a glass capillary microfluidic device. The glass capillary device is assembled with two tapered cylindrical capillaries from opposite sides within a square glass capillary. The cylindrical capillary with a smaller tip, treated with trichloro(1H,1H,2H,2H-perfluorooctyl)silane to be fluorophilic, acts as an inlet for the inner water-PVA phase. The cylindrical capillary with a larger tip, treated with 2-[Methoxy(polyethyleneoxy) 6-9propyl] trimethoxysilane to be hydrophilic, serves as the outlet for the continuous phase. The middle phase consisting of hydrocarbon-fluorocarbon mixture with FBA surfactants is injected through the interstitial space between the inlet and square capillaries, whereas the outer water-PVA phase is injected through the interstitial space between the outlet and square capillaries, as depicted in Figure 4a. Water-in-oil-in-water double emulsion droplets are generated between the two tapered orifices when the three fluid phases meet, as shown in Figure 4b and Video SV2. Hexane and PFH exhibit temperature-dependent miscibility with an UCST around 23 ºC. Thus, the two oil-shell components undergo phase separation upon cooling of the double emulsion droplets from room temperature (RT) to ~0 ºC (ice bath), leading to the formation of a new droplet morphology. Before cooling, the droplets exhibit a core-shell double emulsion structure, as shown in the bright-field and fluorescent microscopy images of the emulsions at room temperature in Figure 4c. Upon cooling, hexane drops initially nucleate and grow in the PFH shell, as shown in Supporting Video SV3. After coarsening, the hexane phase, dyed with Nile Red, deforms into a helmet shape buckled around the inner water core, with both phases engulfed by the PFH phase. This morphology is visualized by the bright-field image of the droplets incubated at 0 ºC in Figure 4c. The position of the hexane phase after droplet phase separation is further demonstrated by the fluorescent microscopy images in Figure 4c with a focus on the crescent-shaped central plane. Due to the interfacial film formation at both the inner and outer water/oil interfaces in the double emulsions, the phase separation of the hexane and PFH is robustly confined within two solid spherical water/oil interfaces. The combination of this micro-confinement and the low hexane-PFH interfacial tension leads to the morphological reconfiguration of the droplets into lower-symmetry two-core triple emulsion drops, as depicted in the rightmost schematic in Figure 4c.

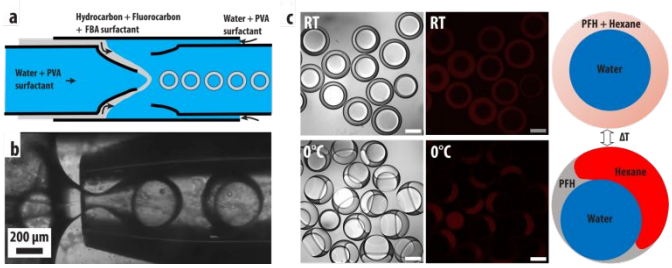


**Figure 4.** (a) Illustration of microfluidic fabrication of the reconfigurable hydrocarbon-fluorocarbon double emulsions. (b) Optical microscopy image of the double emulsion droplet template formation in a glass capillary microfluidic drop maker. (c) Bright-field, fluorescent microscopy images and structure schematics of the reconfigurable hexane-perfluorohexane double emulsion at room temperature and around 0 ºC. The hexane phase is dyed with 1 mg $ml^{-1}$ Nile Red.

## 4. Conclusions

In conclusion, we report the synthesis of the FBA copolymer surfactant and the use of it for the fabrication of reconfigurable hydrocarbon-fluorocarbon double emulsions. Fluoroacrylate and boronic acid acrylamide monomers are copolymerized to form the FBA surfactant, whose boronic acid groups covalently bonded with diols or polyols to produce a solid elastic interfacial film. The FBA surfactant is further used in a hydrocarbon-fluorocarbon mixture as oil phase with PVA in the water phase to generate water-in-oil-in-water double emulsions. The hydrocarbon and fluorocarbon undergo phase separation confined within the two solid elastic water/oil interfaces of the double emulsions upon temperature change, leading to thermally induced morphology reconfiguration of the droplets. The newly designed FBA copolymer surfactant provides a way to prevent drop recoalescence for emulsion stabilization, which would potentially enable new opportunities for many techniques and applications based on fluorinated drops.

## Data availability

Data supporting this article have been included as part of the ESI.

## Conflicts of interest

There are no conflicts to declare.

## Acknowledgements

This work was supported by the National Science Foundation through the Harvard University MRSEC (DMR-2011754). This work was performed in part at the Center for Nanoscale Systems (CNS), a member of the National Nanotechnology Coordinated Infrastructure Network (NNCI), which was

supported by the National Science Foundation under NSF award no. 1541959. CNS is part of Harvard University. Also, we thank Benjamin Thorne and CNS staff Dr. Nicholas S. Colella for assistance with the interfacial rheology.

## References

1 R. Fan, J. Wu, S. Duan, L. Jin, H. Zhang, C. Zhang and A. Zheng, *Int. J. Pharm.*, 2024, **663**, 124551.
2 B. Li, X. Ma, J. Cheng, T. Tian, J. Guo, Y. Wang and L. Pang, *Front. Bioeng. Biotechnol.*, 2023, **11**, 1121870.
3 M. Naz, L. Zhang, C. Chen, S. Yang, H. Dou, S. Mann and J. Li, *Commun. Chem.*, 2024, **7**, 79.
4 N. M. Kovalchuk and M. J. H. Simmons, *Adv. Colloid Interface Sci.* 2023, **312**, 102844.
5 J. Waeterschoot, E. Kayahan, J. Breukers, J. Lammertyn and X. C. Solvas, *RSC Adv.*, 2024, **14**, 24115–24129.
6 J.-C. Baret, *Lab Chip*, 2012, **12**, 422-433.
7 S. Narayan, A. E. Metaxa, R. Bachnak and T. Neumiller, *Curr. Opin. Colloid Interface Sci.*, 2020, **50**, 101385.
8 F. Goodarzi and S. Zendehboudi, *Can. J. Chem. Eng.*, 2018, **97**, 281-309.
9 H.-J. Butt, K. Graf and M. Kappl, *Physics and Chemistry of Interfaces*, Weinheim, Germany, 2003.
10 K. Holmberg, Curr. Opin. Colloid Interface Sci., 2001, **6**, 148–159.
11 M. Andersson Trojer, A. Mohamed and J. Eastoe, *Colloids Surf. A: Physicochem. Eng. Asp.*, 2013, **436**, 1048–1059.
12 A. Veeramanoharan and S. C. Kim, *RSC Adv.*, 2024, **14**, 25429-25471.
13 R. A. Orizondo, D. L. Nelson, M. L. Fabiilli and K. E. Cook, *Colloid Polym Sci.*, 2017, **295**, 2413–2422.
14 R. Zhou, Y. Jin, Y. Shen, P. Zhao and Y. Zhou, J. *Leather Sci. Eng.*, 2021, **3**, 6.
15 M. Sagisaka, T. Fujii, Y. Ozaki, S. Yoda, Y. Takebayashi, Y. Kondo, N. Yoshino, H. Sakai, M. Abe and K. Otake, *Langmuir*, 2004, **20**, 2560–2566.
16 A. Stefanek, K. Łęczycka-Wilk, S. Czarnocka-Śniadała, W. Frąckowiak, J. Graffstein, A. Ryżko, A. Nowak and T. Ciach, *Colloids Surf. B Biointerfaces*, 2021, **200**, 111603.
17 S. M. S. Hussain, A. A. Adewunmi, A. Mahboob, M. Murtaza, X. Zhou and M. S. Kamal, *Adv. Colloid Interface Sci.*, 2022, 303, 102634.
18 M. Pabon and J. M. Corpart, *J. Fluor. Chem.*, 2002, **114**, 149-156.
19 P. Gruner, B. Riechers, L. A. Chacòn Orellana, Q. Brosseau, F. Maes, T. Beneyton, D. Pekin and J. C. Baret, *Curr. Opin. Colloid Interface Sci.*, 2015, **20**, 183–191.
20 J. N. Lee, C. Park and G. M. Whitesides, *Anal. Chem.*, 2003, **75**, 6544–6554.
21 X. Li, S. Y. Tang, Y. Zhang, J. Zhu, H. Forgham, C. X. Zhao, C. Zhang, T. P. Davis and R. Qiao, *Angew. Chem., Int. Ed. Engl.*, 2024, **63**, e202315552.
22 M. S. Chowdhury, W. Zheng, S. Kumari, J. Heyman, X. Zhang, P. Dey and D. A. Weitz, *Nat. Commun.*, 2019, **10**, 4546-4556.
23 R. C. Buck, P. M. Murphy and M. Pabon, Chemistry, Properties, and Use of Commercial Fluorinated Surfactants, in *The Handbook of Environmental Chemistry – Polyfluorinated Chemicals and Transformation Products*, ed. T. P. Knepper and F. T. Lange, Springer Berlin Heidelberg, 2012, vol. 17, pp. 1-24.
24 P. L. Nostro, L. Scalise and P. Baglioni, *J. Chem. Eng. Data.*, 2005, **50**, 1148-1152.
25 P. L. Nostro, *Adv. Colloid Interface Sci.*, 1995, **56**, 245-287.
26 L. D. Zarzar, V. Sresht, E. M. Sletten, J. A. Kalow, D. Blankschtein and T. M. Swager, *Nature*, 2015, 518, 520–524.
27 R. V. Balaj and L. D. Zarzar, *Chem. Phys. Rev.*, 2020, 1, 011301-011327.
28 R. V. Balaj, S. W. Cho, P. Singh and L. D. Zarzar, *Polym. Chem.*, 2020, 11, 281-286.
29 A. E. Goodling, S. Nagelberg, B. Kaehr, C. H. Meredith, S. I. Cheon, A. P. Saunders, M. Kolle and L. D. Zarzar, *Nature*, 2019, 566, 523–527.
30 K. H. Ku, B. R. McDonald, H. Vijayamohanan, C. A. Zentner, S. Nagelberg, M. Kolle and T. M. Swager, *Small*, 2021, **17**, 2007507.
31 S. Nagelberg, L. D. Zarzar, N. Nicolas, K. Subramanian, J. A. Kalow, V. Sresht, D. Blankschtein, G. Barbastathis, M. Kreysing, T. M. Swager and M. Kolle, *Nat. Commun.*, 2017, **8**, 14673.
32 L. Zeininger, S. Nagelberg, K. S. Harvey, S. Savagatrup, M. B. Herbert, K. Yoshinaga, J. A. Capobianco, M. Kolle and T. M. Swager, *ACS Cent. Sci.*, 2019, **5**, 789–795.
33 D. Wei, N. Yin, D. Xu, L. Ge and R. Guo, *ACS Sustainable Chem. Eng.*, 2024, **12**, 5129–5138.
34 S. Nagelberg, J. F. Totz, M. Mittasch, V. Sresht, L. Zeininger, T. M. Swager, M. Kreysing and M. Kolle, *Phys. Rev. Lett.*, 2021, **127**, 144503.
35 X. Wang, Y. Zhou, Y.-K. Kim, M. Tsuei, Y. Yang, J. J. de Pablo and N. L. Abbott, *Soft Matter*, 2019, **15**, 2580-2590.
36 A. Terrel, S. D. Moral, A. Martínez-Bueno and A. Concellón, *Liq. Cryst.*, 2024, **51**, 2321-2338.
37 X. Wang, Y. Zhou, V. Palacio-Betancur, Y.-K. Kim, L. Delalande, M. Tsuei, Y. Yang, J. J. Pablo and N. L. Abbott, *Langmuir*, 2019, **35**, 16312–16323.
38 S. Vandebril, A. Franck, G. G. Fuller, P. Moldenaers and J. Vermant, *Rheol Acta.*, 2010, **49**, 131-144.
39 E. Huang, A. Skoufis, T. Denning, J. Qi, R. Dagastine, R. Tabor and J. Berry, *J. Open Source Softw.* 2021, **6**, 2604.
40 R. K. Shah, H. C. Shum, A. C. Rowat, D. Lee, J. J. Agresti, A. S. Utada, L.-Y. Chu, J.-W. Kim, A. Fernandez-Nieves, C. J. Martinez and D. A. Weitz, *Mater. Today,* 2008, **11**, 18-27.
41 A. S. Utada, E. Lorenceau, D. R. Link, P. D. Kaplan, H. A. Stone and Weitz, D. A. *Science*, 2005, **308**, 537–541.
42 S. S. Datta, A. Abbaspourrad, E. Amstad, J. Fan, S. H. Kim, M. Romanowsky, H. C. Shum, B. Sun, A. S. Utada, M. Windbergs, S. Zhou, and D. A. Weitz, *Adv. Mater*. 2014, **26**, 2205–2218.
43 J. K. Nunes, S. S. H. Tsai, J. Wan and H. A. Stone, *J. Phys. D: Appl. Phys.* 2013, **46***, 114002*.
44 A. S. Utada, L.-Y. Chu, A. Fernandez-Nieves, D. R. Link, C. Holtze and D. A. Weitz, *MRS Bulletin*, 2007, **32**, 702-708.
45 B. Xianyu and H. Xu, *Supermol.*, 2024, **3**, 100070-100080.
46 H. Wang, D. Zhu, A. Paul, L. Cai, A. Enejder, F. Yang and S. C. Heilshorn, *Adv. Funct. Mater.*, 2017, **27**, 1605609.
47 C. Loebel, C. B. Rodell, M. H. Chen and J. A. Burdick, *Nat. Protoc.*, 2017, **12**, 1521-1541.
48 T-C. Tseng, L. Tao, F-Y. Hsieh, Y. Wei, I-M. Chiu and S-H. Hsu, *Adv. Mater.*, 2015, **27**, 3518-3524.
49 S. Uman, A. Dhand and J. A. Burdick, *J. Appl. Polym. Sci.*, 2020, **137**, 48668-48687.
50 L. Voorhaara and R. Hoogenboom, *Chem. Soc. Rev.*, 2016, **45**, 4013-4031.

**Data Availability Statement**

The data supporting this article have been included as part of the Supplementary Information.

Supporting Video 1 (SV1): Microfluidic drop generation of the hydrocarbon-fluorocarbon reconfigurable emulsions, 50fps

Supporting Video 2 (SV2): Transient wrinkle formation during retraction of HFE-7500 drop containing 3wt% FBA from 0.08M HEPES, 50fps

Supporting Video 3 (SV3): Droplet morphology reconfiguration during temperature change from RT to 0°C